The Abdus Salam
International Centre for Theoretical Physics

2160-4

Conference on Decadal Predictability

16 - 20 August 2010

Potentially Predictable Patterns of the Tropospheric Circulation in the IPCC-AR4 Multi-model Ensemble

Dörthe Handorf *and Klaus Dethloff*
Alfred-Wegener Institute For Polar & Marine Research
Research Department
Telegrafenberg A43
D-14473 Potsdam
GERMANY

Potentially Predictable Patterns of the Tropospheric Circulation in the IPCC AR4 Multi-model Ensemble

Dörthe Handorf, Klaus Dethloff

Alfred Wegener Institute for Polar and Marine Research
Research Department Potsdam

Trieste, 2010

Atmospheric predictability on seasonal time-scales and beyond

- Considerable atmospheric variability on synoptic time-scales, but also in longer time-scales (seasonal to decadal)
- Longer time-scale atmospheric variability due to:
  - Slowly varying internal dynamics of the atmosphere
  - External forcings for the atmosphere (e.g. SST anomalies, sea-ice distribution, soil moisture, changing GHG concentrations)
  - High-frequency, unpredictable weather variability

→ Monthly/seasonally averaged atmospheric anomalies due to weather noise are unpredictable beyond the first two weeks

- Potential predictability beyond the limit of deterministic weather predictability can be defined as the difference between the total variance of the monthly/seasonally averaged atmospheric anomalies minus the variance, attributed to the weather noise (Madden, 1976)

Patterns of atmospheric variability – Teleconnections I

- **Teleconnection patterns →**
  - refer to recurring and persistent, large-scale patterns of pressure and circulation anomalies that spans vast geographical areas
  - localised in definite regions
  - govern the variability in our climate system on a broad range of time and spatial scales, e.g. the decadal behavior of NAO
  - often determined by
    Correlation or Empirical Orthogonal Function Analysis

Patterns of atmospheric variability – Teleconnections II

Comparison of spatial pattern of simulated NAO, Taylordiagram for 23 IPCC models, 1958-1999

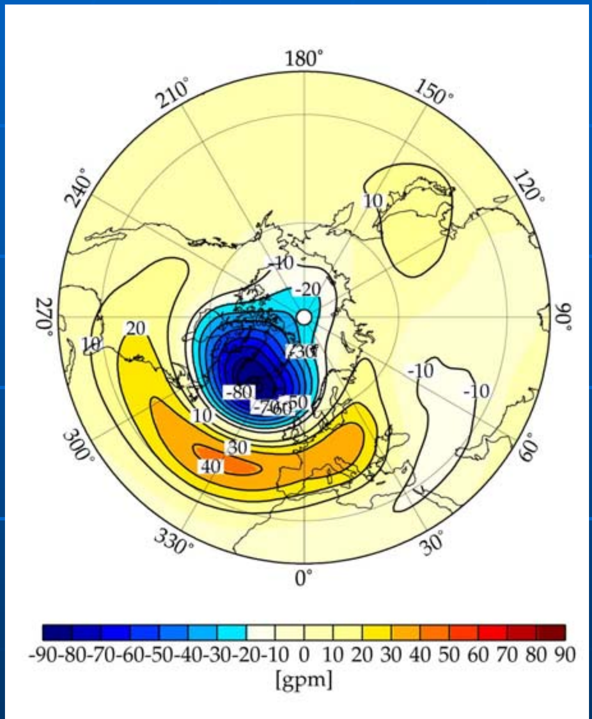

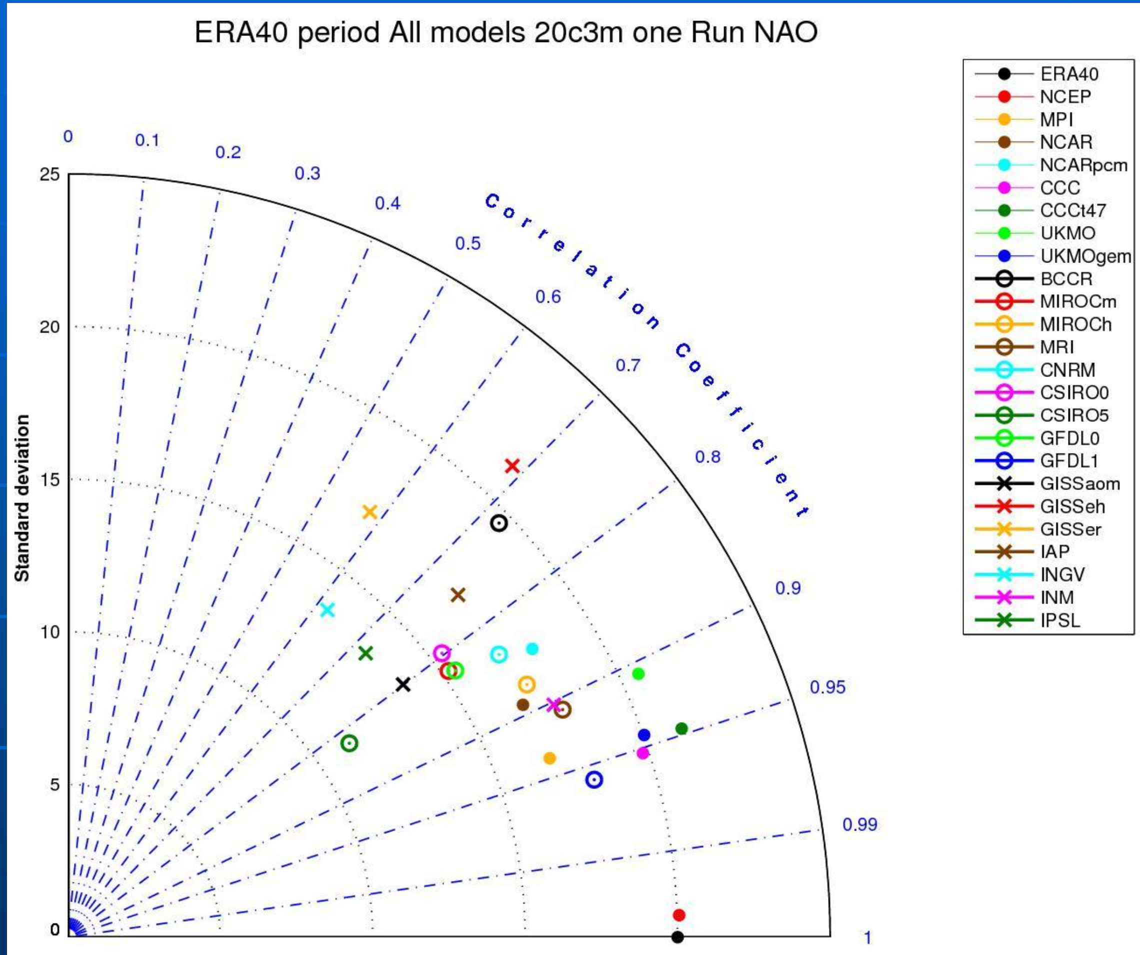

- ➢ Teleconnections in the extra-tropics are largely determined by the weather-noise component
  → the predictive skill in the extratropics may be limited to 1 or 2 weeks

Patterns of potential predictability

➢ Teleconnections in the extra-tropics are largely determined by the weather-noise component → limited predictive skill

➢ Which patterns capture the **potentially predictable component** of variability on longer time-scales?

➢ How well reproduce state-of-the-art GCMs these **potentially predictable patterns**?

Determination of patterns of potential predictability
which are closely related to slowly varying external forcings and internal dynamics

Application of the method introduced by Zheng and Frederiksen (2004)

Patterns of potential predictability

Method introduced by Zheng and Frederiksen (2004)

→ is based on the Analysis of Variance (ANOVA)

→ can be considered as **diagnostic estimation of predictability**

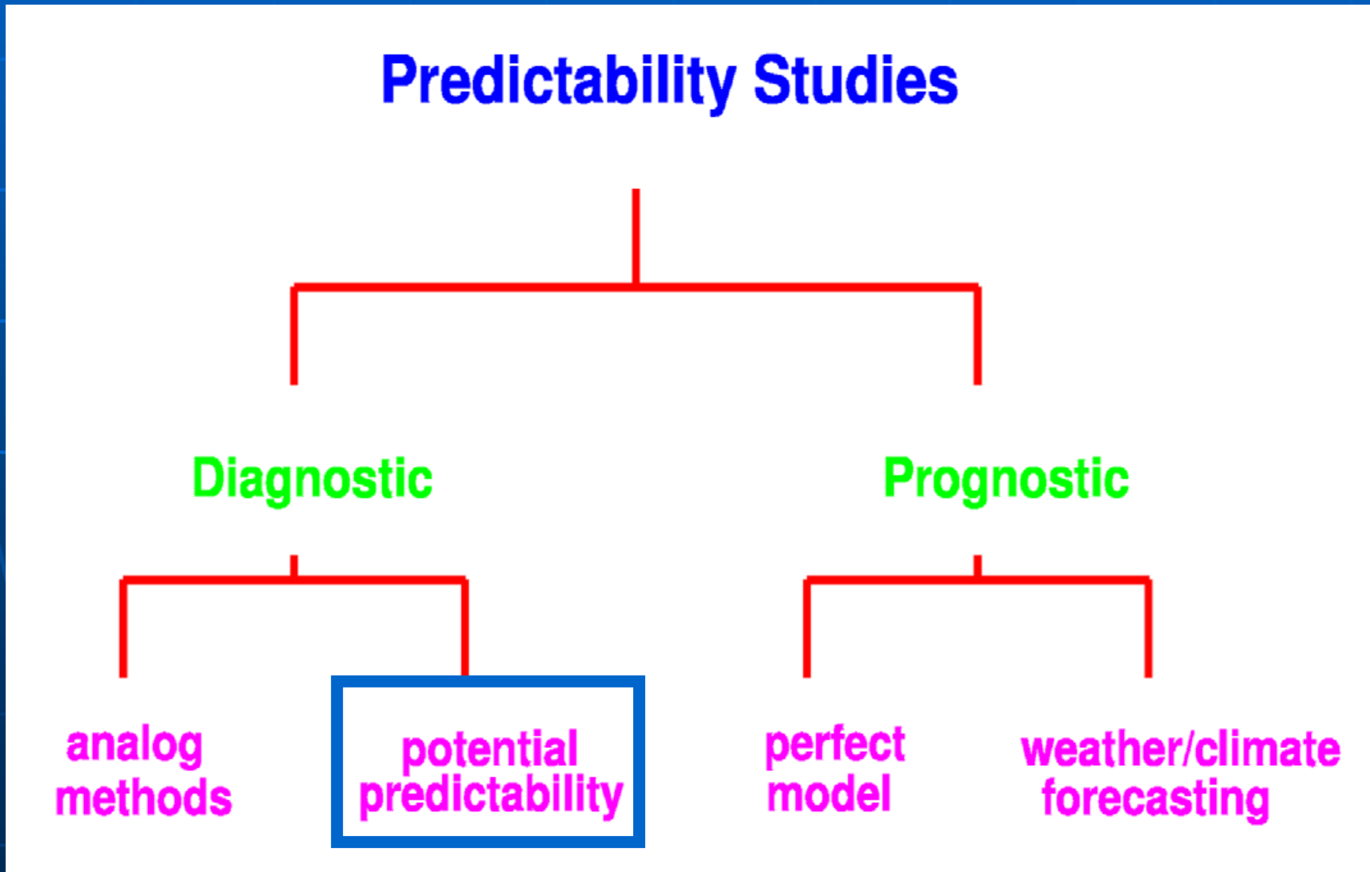

G.J. Boer (2008), Presentation at 12th Session of the WCRP/CLIVAR Working Group on Coupled Modelling

Potentially Predictable Patterns

(Zheng and Frederiksen, Clim. Dyn., 2004)

➢ Idea: Decomposition of meteorological fields into a slow component (due to long-term variability by external forcing and slow internal dynamics) and a intraseasonal component (due to weather variability)

➢ Proposal of a modified EOF analysis
→ Determination of patterns of interannual variability of seasonal means that arise from intraseasonal variability
→ After removing this component, estimation of the long-range potentially predictable patterns

➢ Proposed method is using monthly means of climate data
→ more computationally efficient than methods that use daily means

➢ Spatial patterns derived by this modified EOF analysis are more potentially predictable than those derived by the conventional EOF analysis or rotations of EOFs (Frederiksen and Zheng, 2004)

Potentially Predictable Patterns - Statistical Model

- Let $x_{ym}(r)$ be a monthly anomaly of a climate variable from the mean annual cycle at geographical location r
- $m=1,2,3$ month number; $y=1,\ldots,Y$ year number; $r=1,\ldots,R$ location index
- Consider the decomposition (1-way ANOVA)

$$x_{ym}(r) = \mu_y(r) + \varepsilon_{ym}(r)$$

- $\mu_y(r)$: seasonal population mean anomal in year y

  due to slowly varying external forcings and internal dynamics

  Slow climate signal on (interannual and longer) time-scale

- $\varepsilon_{ym}(r)$: residual monthly departure

  arises from intraseasonal variability

  Intraseasonal weather noise

Determination of Potentially Predictable Patterns

(Zheng and Frederiksen, Clim. Dyn., 2004)

- Basic statistical model: A seasonal mean anomaly can be expressed as

$$x_{yo}(r) = \mu_y(r) + \varepsilon_{yo}(r)$$

- Index o represents an average taken over that independent variable (e.g. for seasonal means average over m

- Estimate of the interannual covariance of the intraseasonal weather noise component is derived by Zheng and Frederiksen (2004):

$$\hat{V}(\varepsilon_{yo}(r_1), \varepsilon_{yo}(r_2)) = \hat{\sigma}(3 + 4\hat{\phi})/9 \qquad \textbf{(1)}$$

$$\hat{\sigma} = a + b$$

$$\hat{\phi} = \frac{a + 2b}{2(a+b)}$$

$$a = \frac{1}{2}\left\{\frac{1}{Y}\sum_{y=1}^{Y}\left(x_{y1}(r_1) - x_{y2}(r_1)\right)\left(x_{y1}(r_2) - x_{y2}(r_2)\right) + \frac{1}{Y}\sum_{y=1}^{Y}\left(x_{y2}(r_1) - x_{y3}(r_1)\right)\left(x_{y2}(r_2) - x_{y3}(r_2)\right)\right\}$$

$$b = \frac{1}{2}\left\{\frac{1}{Y}\sum_{y=1}^{Y}\left(x_{y1}(r_1) - x_{y2}(r_1)\right)\left(x_{y2}(r_2) - x_{y3}(r_2)\right) + \frac{1}{Y}\sum_{y=1}^{Y}\left(x_{y2}(r_1) - x_{y3}(r_1)\right)\left(x_{y1}(r_2) - x_{y2}(r_2)\right)\right\}$$

Determination of Potentially Predictable Patterns

(Zheng and Frederiksen, Clim. Dyn., 2004)

- Estimate of the interannual covariance between seasonal means given by

$$\hat{V}(x_{yo}(r_1), x_{yo}(r_2)) = \frac{1}{Y-1}\sum_{y=1}^{Y}\left(x_{yo}(r_1) - x_{oo}(r_1)\right)\left(x_{yo}(r_2) - x_{oo}(r_2)\right) \quad \textbf{(2)}$$

- Residual covariance after removing the intraseasonal variability:

$$\hat{V}(x_{yo}(r_1), x_{yo}(r_2)) - \hat{V}(\varepsilon_{yo}(r_1), \varepsilon_{yo}(r_2)) =$$
$$\hat{V}(\mu_y(r_1), \mu_y(r_2)) + \hat{V}(\mu_y(r_1), \varepsilon_{yo}(r_2)) + \hat{V}(\varepsilon_{yo}(r_1), \mu_y(r_2))$$

- If intraseasonal components independent on slow components →

$$\hat{V}(x_{yo}(r_1), x_{yo}(r_2)) - \hat{V}(\varepsilon_{yo}(r_1), \varepsilon_{yo}(r_2)) = \hat{V}(\mu_y(r_1), \mu_y(r_2)) \quad \textbf{(3)}$$

- Not generally valid, but $\hat{V}(x_{yo}(r_1), x_{yo}(r_2)) - \hat{V}(\varepsilon_{yo}(r_1), \varepsilon_{yo}(r_2))$ may still be a better estimate of variability in slow component than is $\hat{V}(x_{yo}(r_1), x_{yo}(r_2))$

Determination of Potentially Predictable Patterns

(Zheng and Frederiksen, J. Clim., 2004)

- Determination of covariance matrices associated with the potentially predictable and weather noise components possible→
- Patterns for each component can be derived by VARIMAX rotated EOF analysis on the basis of the covariance matrices (1) (2) (3)
- Associated principal component time series (PC) for each (rotated) EOF defined as the dot product between $x_{ym}(r)$ and the (rotated) EOF

$$p_{ym} = \sum_{r=1}^{R} eof(r) x_{ym}(r) = \sum_{r=1}^{R} eof(r) \mu_y(r) + \sum_{r=1}^{R} eof(r) \varepsilon_{ym}(r) = \tilde{\mu}_y + \tilde{\varepsilon}_{ym}$$

- Fraction of variance remaining after the removal of the intraseasonal component from the PC time series (residual variance fraction)

$$(1 - V(\tilde{\varepsilon}_{yo}) / V(p_{yo}))$$

Evaluation of Potentially Predictable Patterns: Taylor-Diagrams and Skill Scores

Taylor diagrams (Taylor, 2001)
→ Quantification of similarity between different patterns
→ Compact summary of pattern statistics in terms of pattern correlation, root-mean-square difference and ratio of variances.

Skill score of a model in reproducing a pattern
→ One definition given by Taylor (2001):

$$S = \frac{4(1+R)^4}{\left(\frac{\sigma_f}{\sigma_r} + \frac{\sigma_r}{\sigma_f}\right)^2 (1+R_0)^4}$$

σ_f Standard deviation of test field
σ_r Standard deviation of reference field
R Correlation, R_0 imaximal attainable correlation

This skill score S increases the penalty for low correlation

Potentially predictable patterns:
Analyses of IPCC AR4 model simulations

- Analyses of available monthly mean data
- Analyses of midtropospheric circulation
  - → 500hPa geopotential height fields
- Analyses of dynamically active season of Northern Hemisphere (NH)
  - → December, January, February data (DJF)
- Fields from 20°-90° N
- seasonal cycle removed

For comparison: NCEP/NCAR and ERA40 Reanalysis

IPCC AR4 Coupled Atmosphere-Ocean GCM Simulations

Model	Atmosphere	Ocean	Coupling
BCCR-BCM2.0 Bjerknes Centre for Climate Research, Norway	1.9° x 1.9°	0.5°-1.5° x 1.5°	No flux adjustment
CCSM3 NCAR, USA	1.4° x 1.4°	0.3°-1.0° x 1.0°	No flux adjustment
CGCM3.1 (T47) Canadian Centre for Climate Modeling and Analysis	2.8° x 2.8°	1.9° x 1.9°	No flux adjustment
CGCM3.1 (T63) Canadian Centre for Climate Modeling and Analysis	1.9° x 1.9°	0.9° x 1.4°	No flux adjustment
CNRM-CM3 Meteo-France/Centre National de Recherches Meteorol.	1.9° x 1.9°	0.5°-2.0° x 2.0°	No flux adjustment
CSIRO Mk3.0 CSIRO Atmospheric Research, Australia	1.9° x 1.9°	0.8° x 1.9°	No flux adjustment
CSIRO Mk3.5 CSIRO Atmospheric Research, Australia	1.9° x 1.9°	0.8° x 1.9°	No flux adjustment
ECHAM5/MPI-OM Max Planck Institute Hamburg, Germany	1.9° x 1.9°	1.5° x 1.5°	No flux adjustment
FGOALS-g1.0 Institute of Atmospheric Physics, China	2.8° x 2.8°	1.0° x 1.0°	No flux adjustment
GFDL CM2.0 U.S. Dep.of Commerce/NOAA/GFDL, USA	2.0° x 2.5°	0.3°-1.0° x 1.0°	No flux adjustment
GFDL CM2.1 U.S. Dep.of Commerce/NOAA/GFDL, USA	2.0° x 2.5°	0.3°-1.0° x 1.0°	No flux adjustment
GISS-AOM NASA/Goddard Institute for Space Studies, USA	3° x 4°	3° x 4°	No flux adjustment
GISS-EH NASA/Goddard Institute for Space Studies, USA	4° x 5°	2° x 2°	No flux adjustment
GISS-ER NASA/Goddard Institute for Space Studies, USA	4° x 5°	4° x 5°	No flux adjustment
INGV-SXG Instituto Nazionale di Geofisica e Vulcanologia, Italy	1.1° x 1.1°	1°-2° x 2°	No flux adjustment
INM-CM3.0 Institute for Numerical Mathematics, Russia	4° x 5°	2° x 2.5°	Annual mean flux adjustment of water, no adjustment for heat,mom. fluxes
IPSL CM4 Institut Pierre-Simon Laplace, France	2.5° x 3.75°	2° x 2°	No flux adjustment
MIROC3.2(hires) Center for Climate System Research, National Institute for Environ. Studies, and Frontier Research Center, Japan	1.1° x 1.1°	0.2° x 0.3°	No flux adjustment
MIROC3.2(medres) Japan	2.8° x 2.8°	0.5°-1.4° x 1.4°	No flux adjustment
MRI CGCM2.3.2 Meteorological Research Institute, Japan	2.8° x 2.8°	0.5°-2.0° x 2.5°	Monthly climat. flux adjustment for heat, water and mom. (only 12S-12N)
PCM NCAR, USA	2.81° x 2.81°	0.5°-0.7° x 1.1°	No flux adjustment
UKMO HadCM3 Hadley Centre/ Met Office, UK	2.5° x 3.75°	1.25° x 1.25°	No flux adjustment
UKMO HadGEM1 Hadley Centre/ Met Office, UK	1.3° x 1.9°	0.3°-1.0° x 1.0°	No flux adjustment

IPCC AR4 Coupled Atmosphere-Ocean GCM Simulations Analysed Experiments

20th century simulation (20CM3-CMIP3) 1870-1999 Analyses of years 1958-1999	Anthropogenic forcing: CO2,CH4,N2O, F11,F12,O3,sulfate	23 models
21th22nd century simulation (SRESA1B) 2000-2199 Analyses of years 2000-2099	Anthropogenic forcing: CO2 (about 700ppm by 2100),CH4,N2O, F11F11,F12,O3,sulfate Constant forcing after year 2100	23 models

IPCC AR4 Atmosphere-Only GCM Simulations

20th century simulation (AMIP-style) 1979-1999	Boundary forcing: realistic SST and sea ice Anthropogenic forcing: CO2,CH4,N2O, F11,F12,O3,sulfate	13 models

Seasonal Teleconnection Patterns (Total Field): Reanalysis data ERA40 1958-1999, Winter

REOF1 (20%, 56%)	REOF2 (17%, 48%)	REOF3 (9%, 45%)	REOF4 (9%, 40%)
NAO	PNA	WP	EA

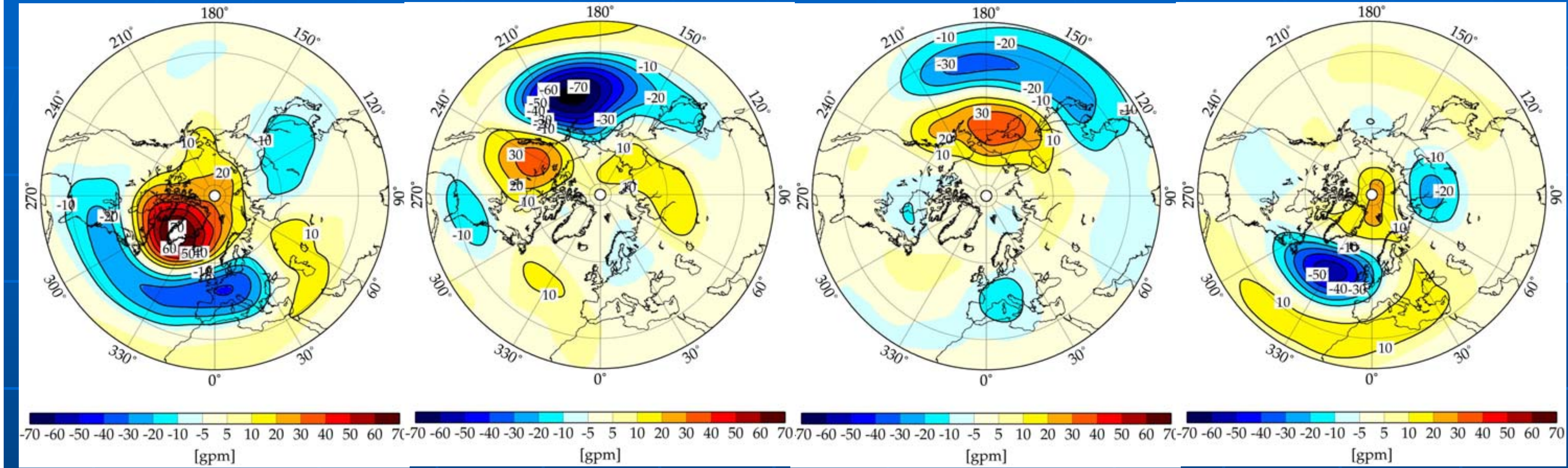

xx% Explained Variance

yy% Residual variance fraction

Intraseasonal Patterns
Reanalysis data ERA40 1958-1999, Winter

REOF1 (15%) REOF2 (14%) REOF4 (6%) REOF5 (6%)

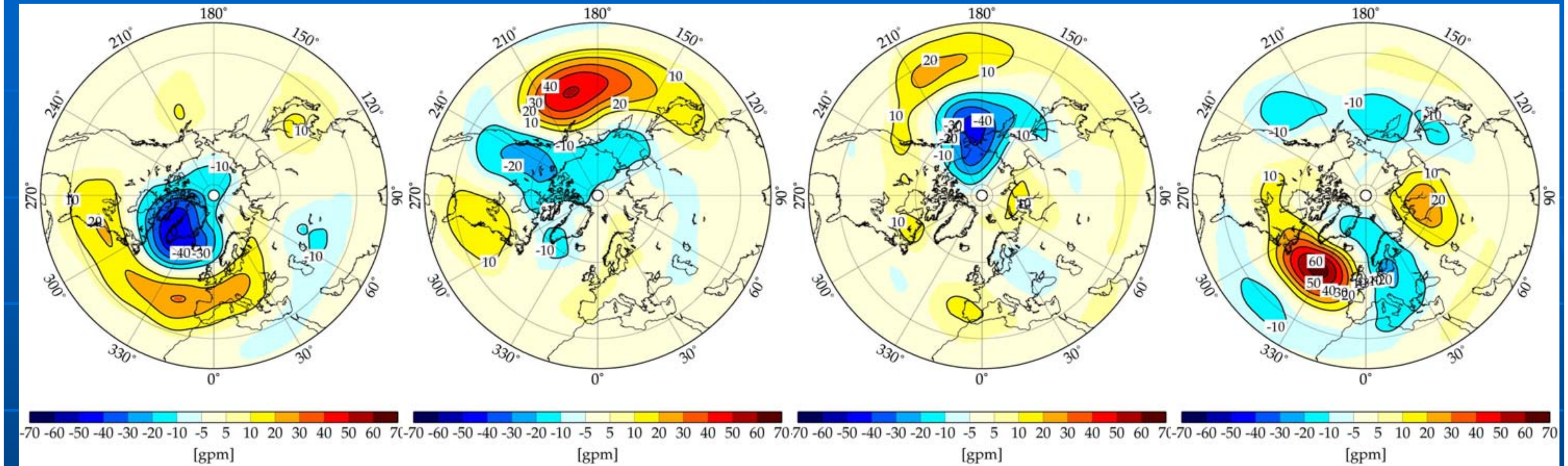

xx% Explained Variance

Slow, Potentially Predictable Patterns: Reanalysis data ERA40 1958-1999, Winter

REOF1 (20%, 68%) EOF2 (14%, 63%) EOF3 (10%, 62%) EOF4 (6%, 68%)

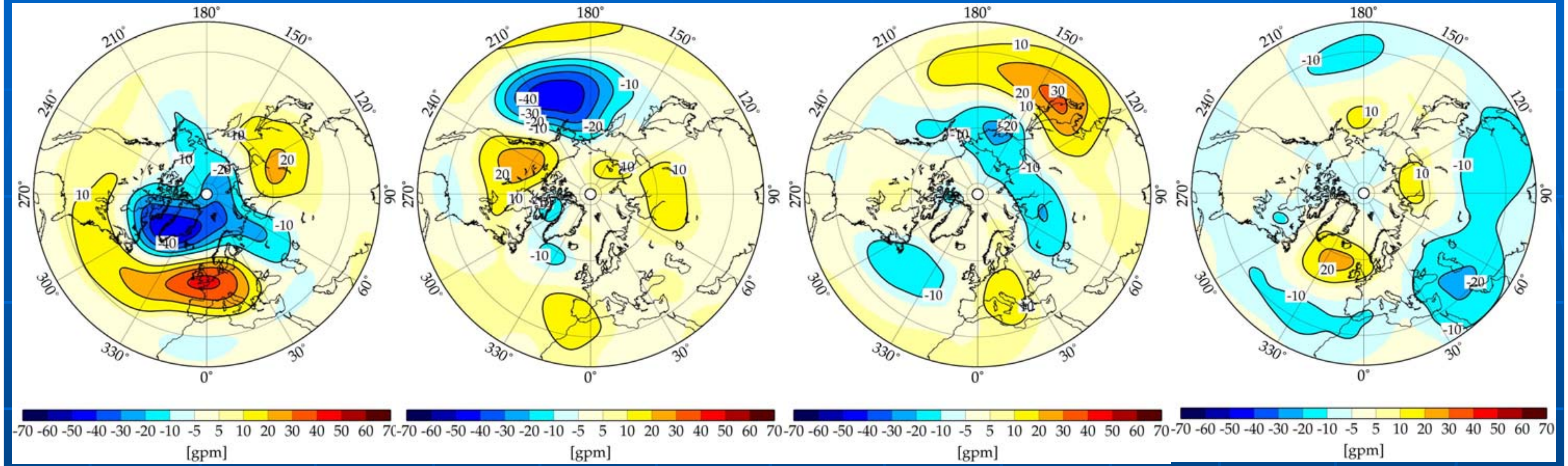

Patterns bear resemblance with

NAO PNA WP EA

xx% Explained Variance

yy% Residual variance fraction

Explained Variance of leading Potentially Predictable Patterns, 23 CMIP models
ERA40 period 1958-1999

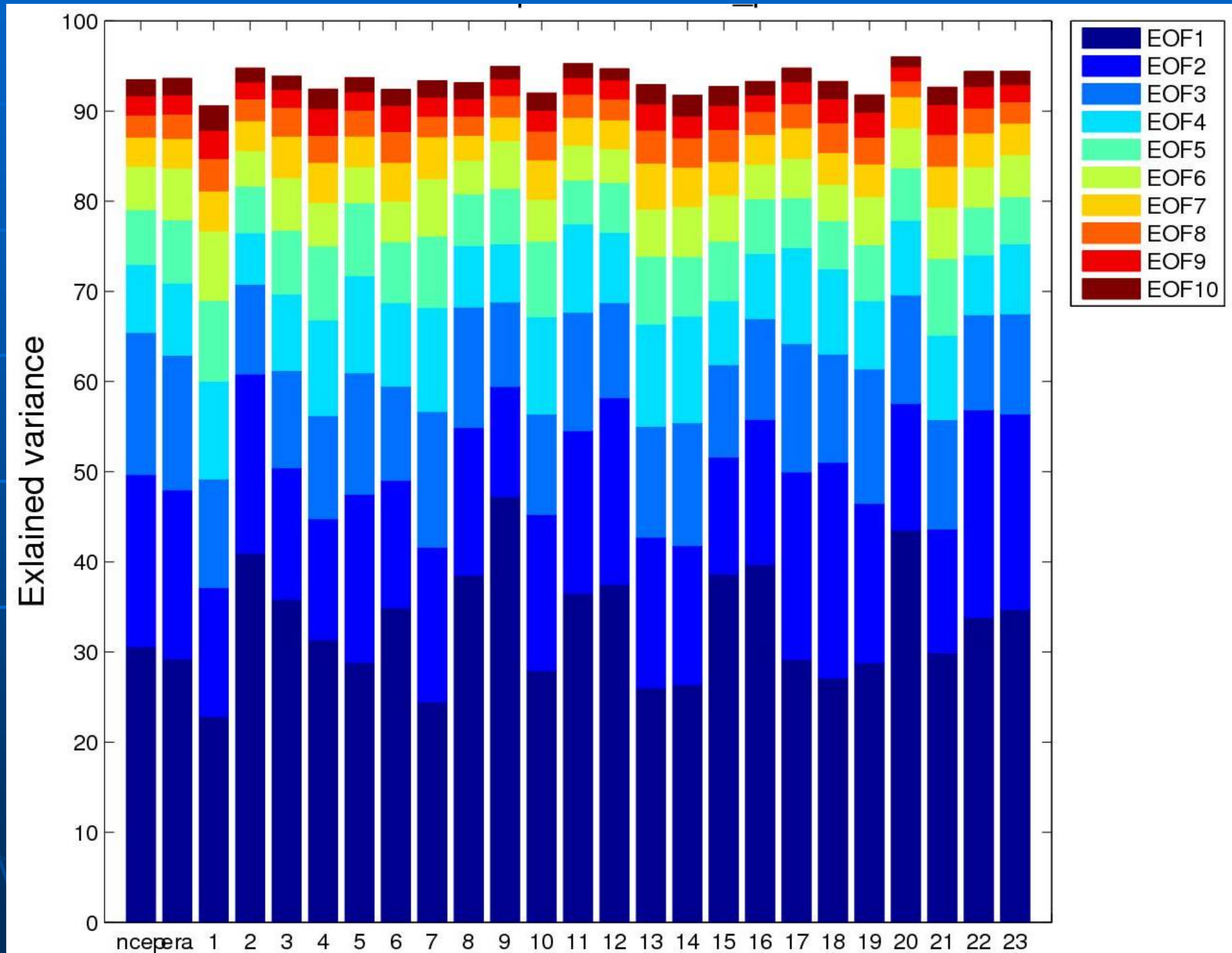

Potentially Predictable Patterns, 23 CMIP models

NAO, ERA40 period 1958-1999

MPI-ECHAM5/OM1 **NCAR-PCM** **UKMO-HadGEM** **MIROC-MEDRES** **IAP**

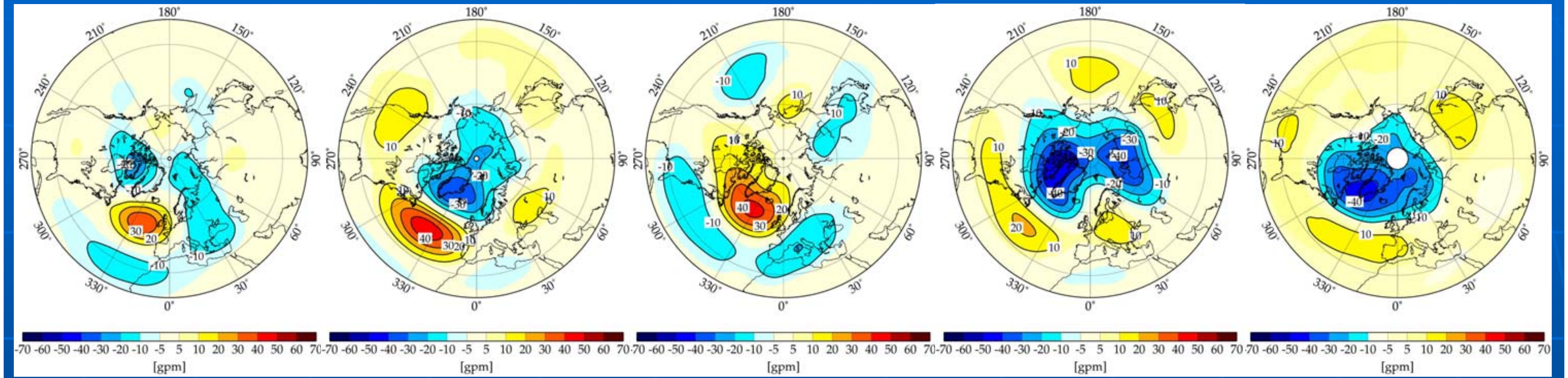

ERA40 **NCEP**

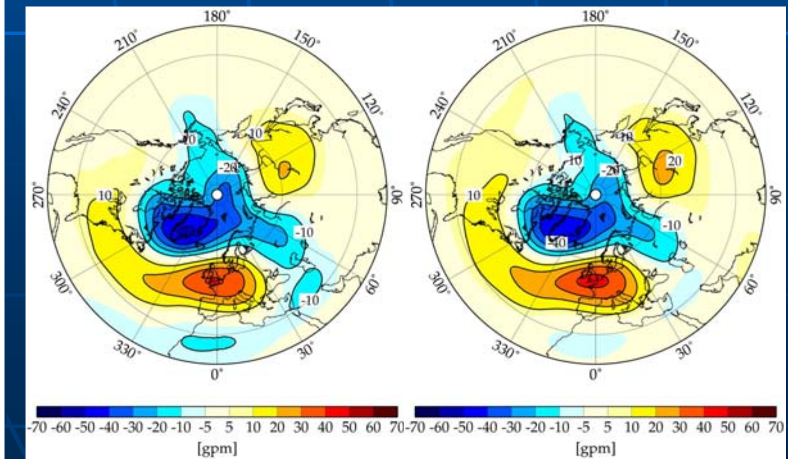

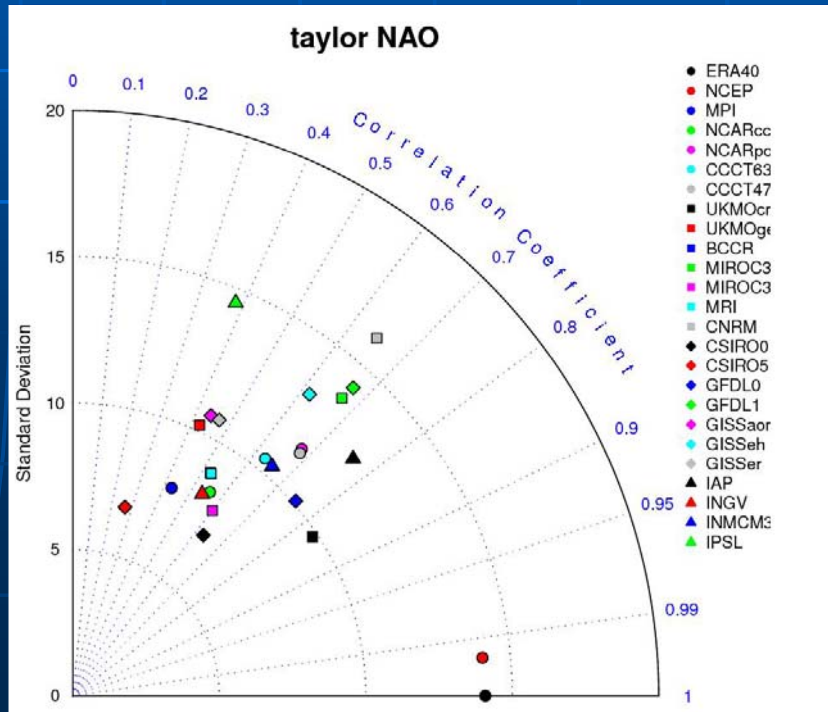

Potentially Predictable Patterns, 23 CMIP models
NAO, ERA40 period 1958-1999

MPI-ECHAM5/OM1 NCAR-PCM UKMO-HadGEM MIROC-MEDRES IAP

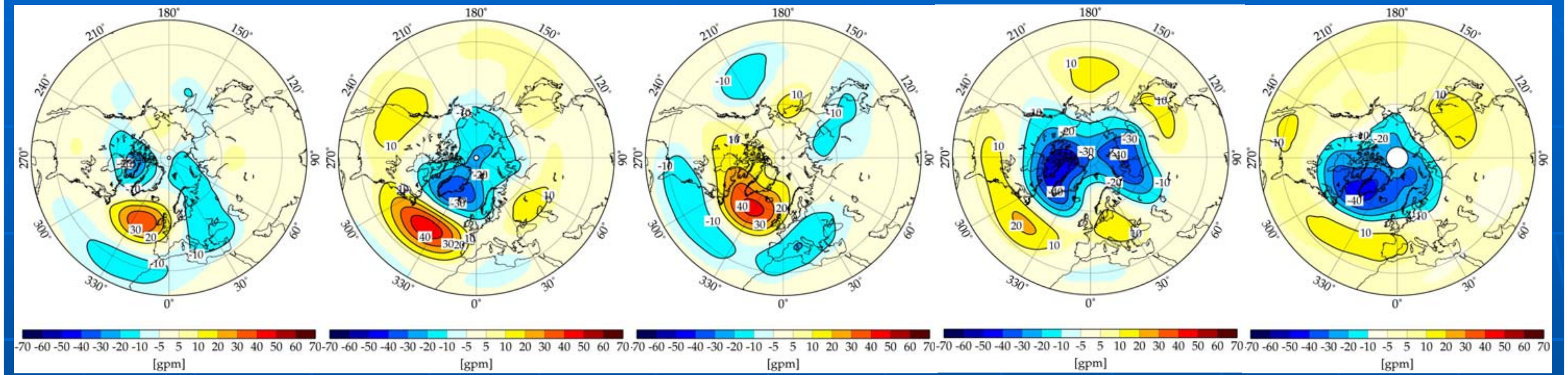

ERA40 NCEP

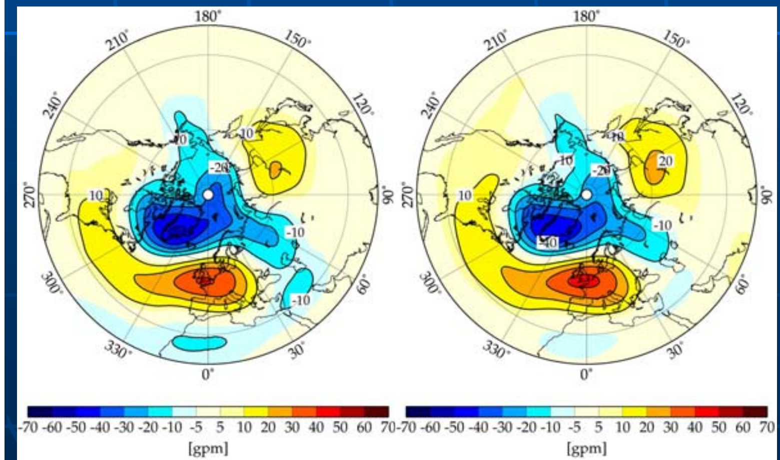

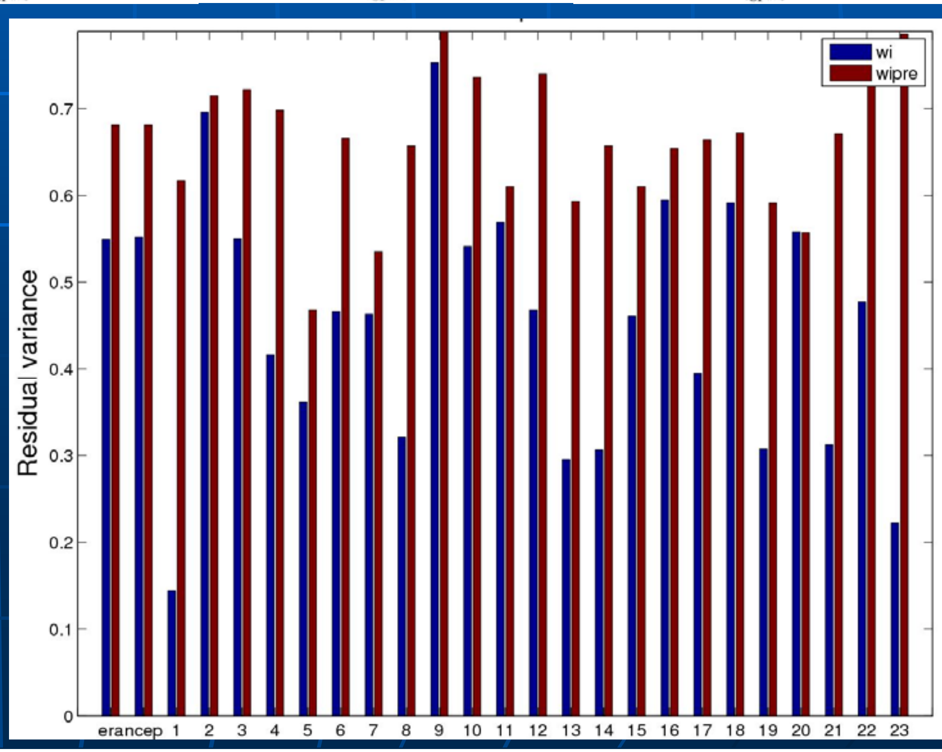

Potentially Predictable Patterns, 23 CMIP models

PNA, ERA40 period 1958-1999

MPI-ECHAM5/OM1 NCAR-PCM UKMO-HadGEM MIROC-MEDRES IAP

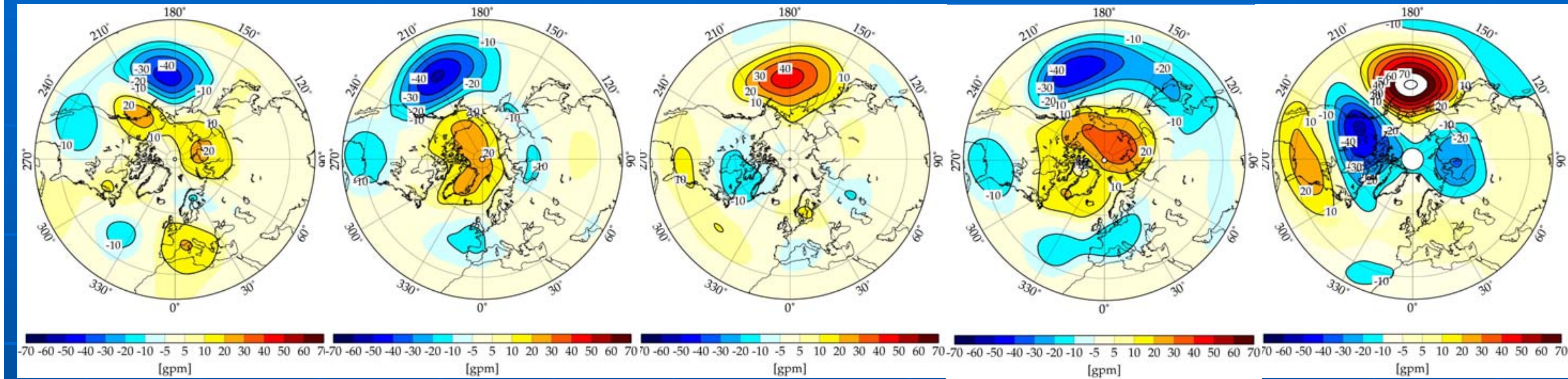

ERA40 NCEP

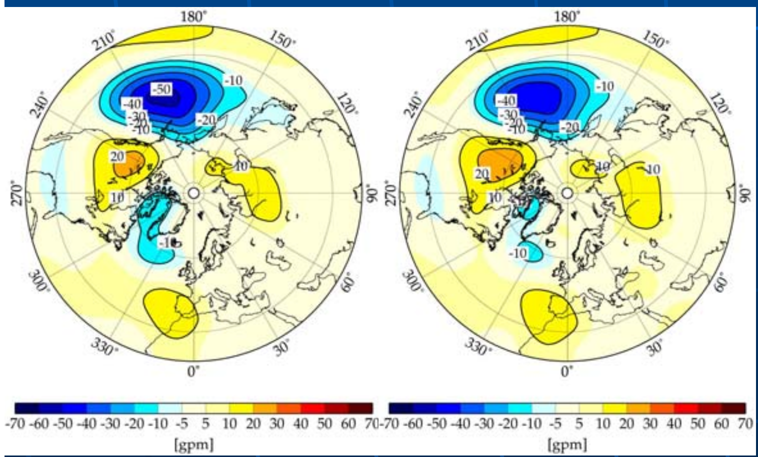

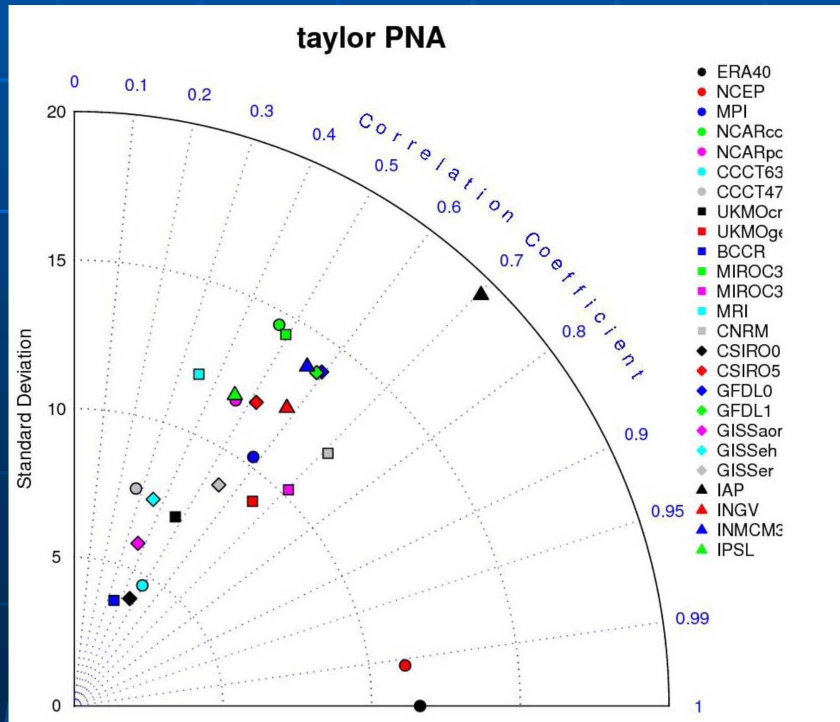

Potentially Predictable Patterns, 23 CMIP models

PNA, ERA40 period 1958-1999

MPI-ECHAM5/OM1 | NCAR-PCM | UKMO-HadGEM | MIROC-MEDRES | IAP

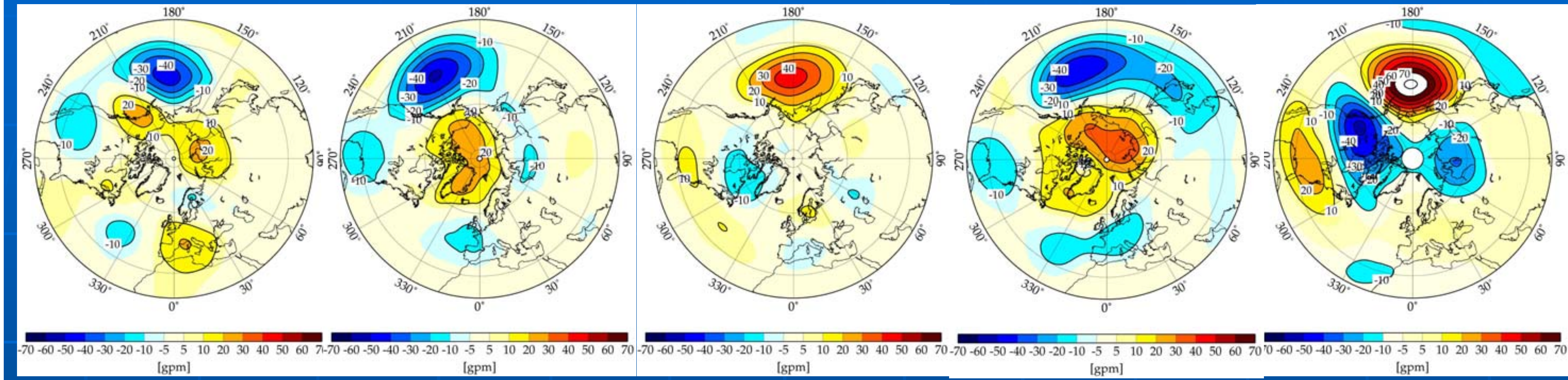

ERA40 | NCEP

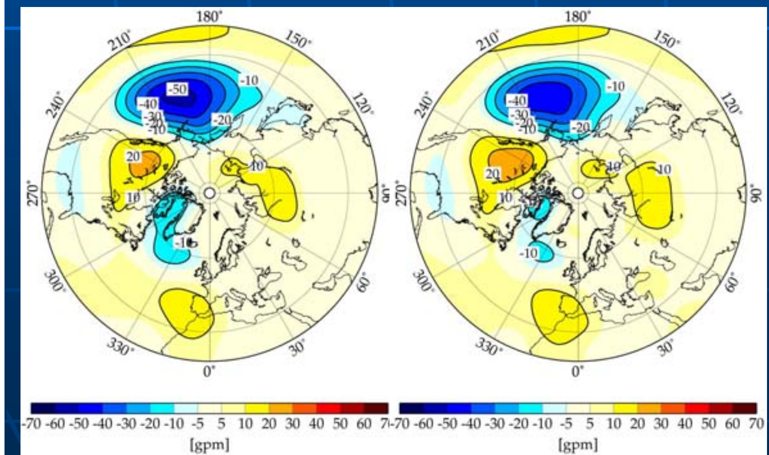

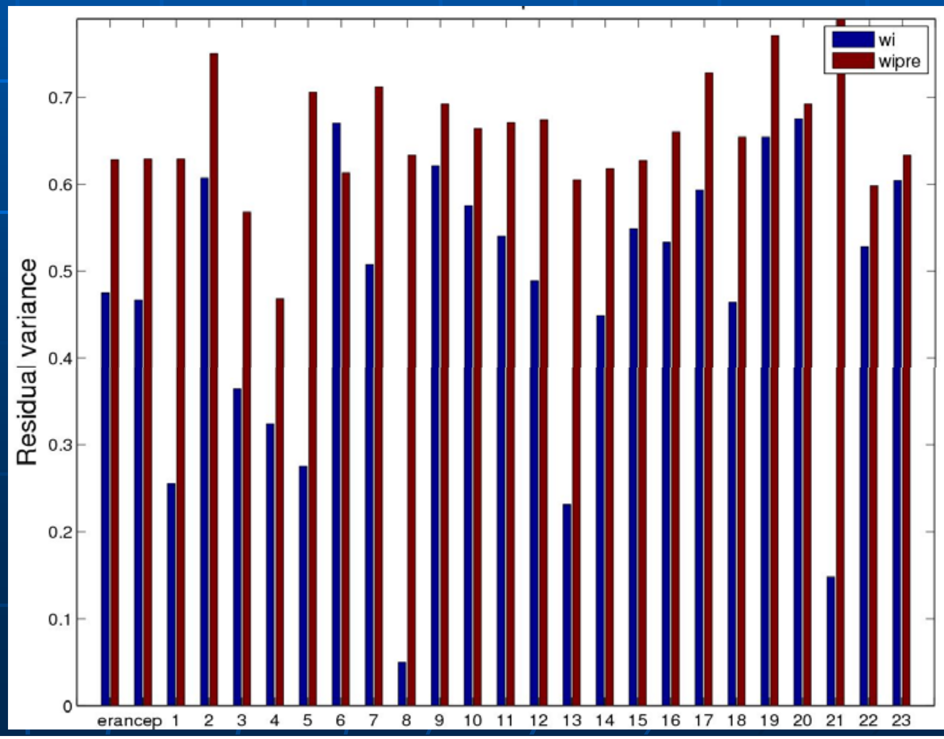

Explained Variance of leading Potentially Predictable Patterns, 13 AMIP models

Period 1979-1999

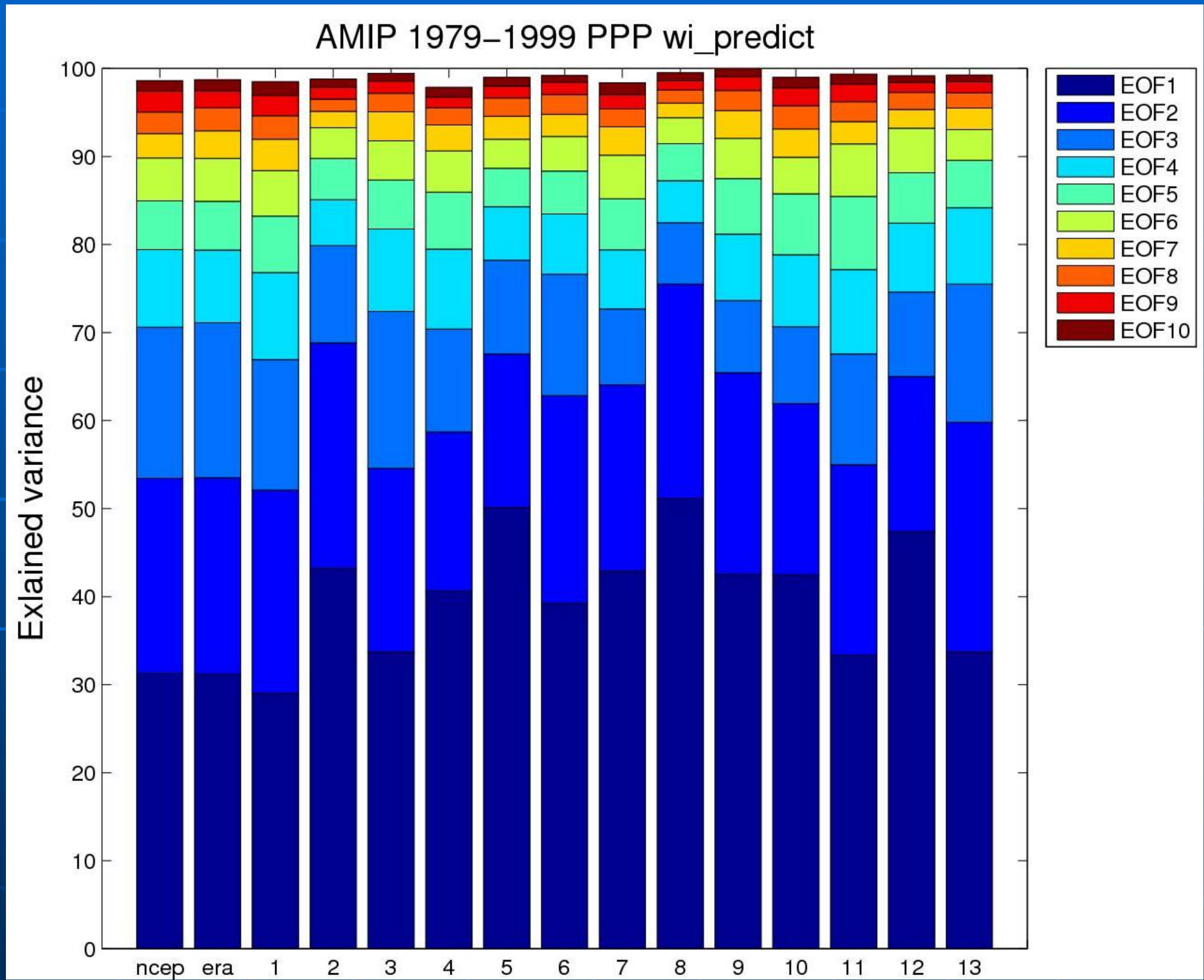

Potentially Predictable Patterns, 13 AMIP models
NAO, Period 1979-1999

MPI-ECHAM5/OM1 NCAR-PCM UKMO-HadGEM MIROC-MEDRES IAP

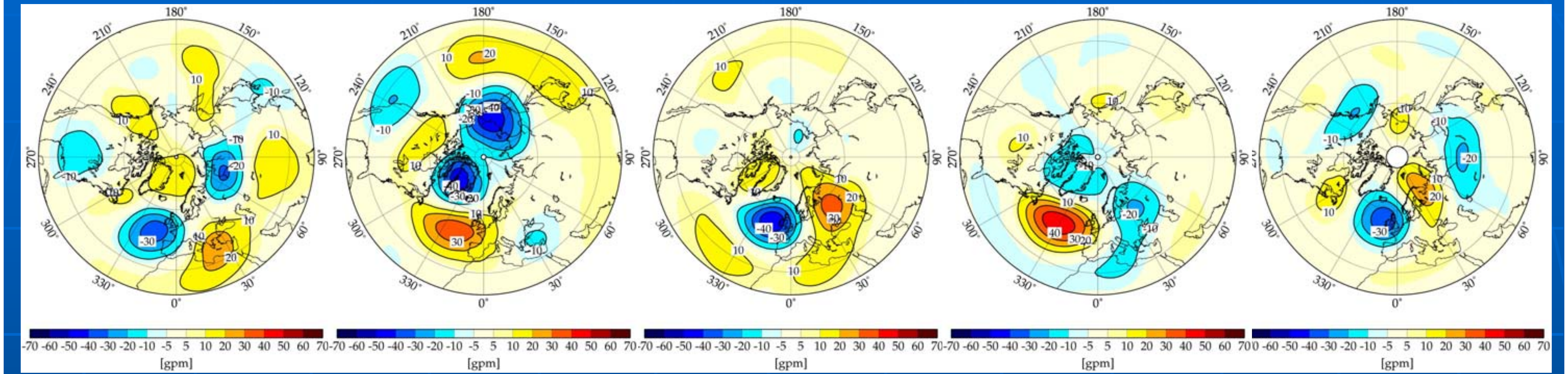

ERA40 NCEP

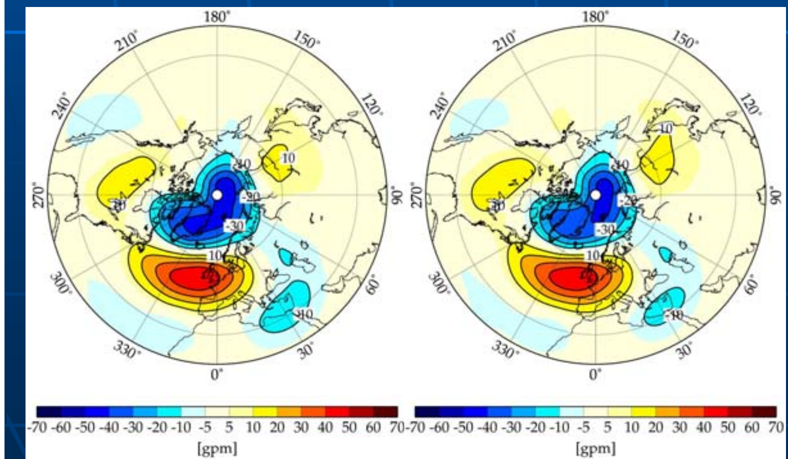

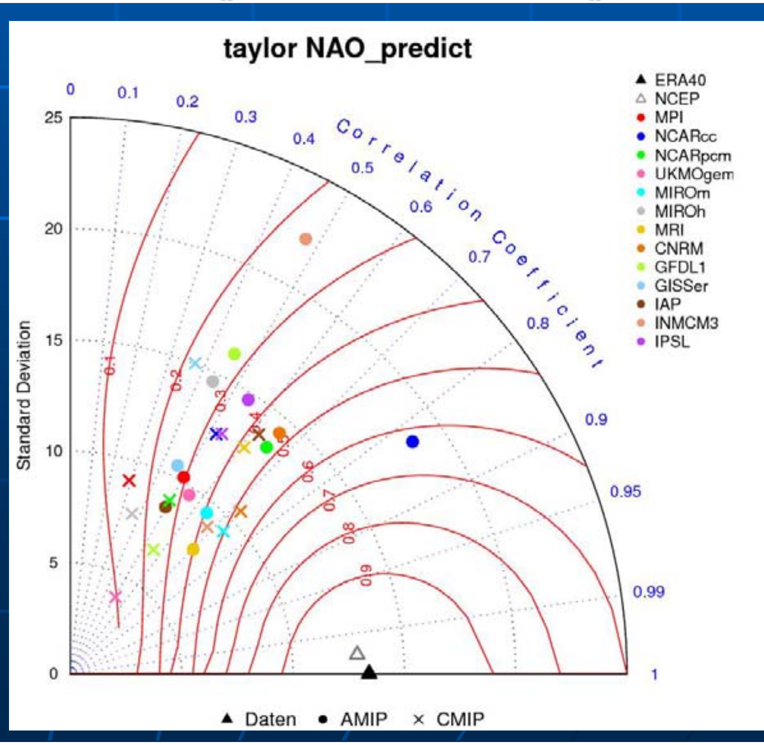

Potentially Predictable Patterns, 13 AMIP models

NAO, Period 1979-1999

MPI-ECHAM5/OM1 NCAR-PCM UKMO-HadGEM MIROC-MEDRES IAP

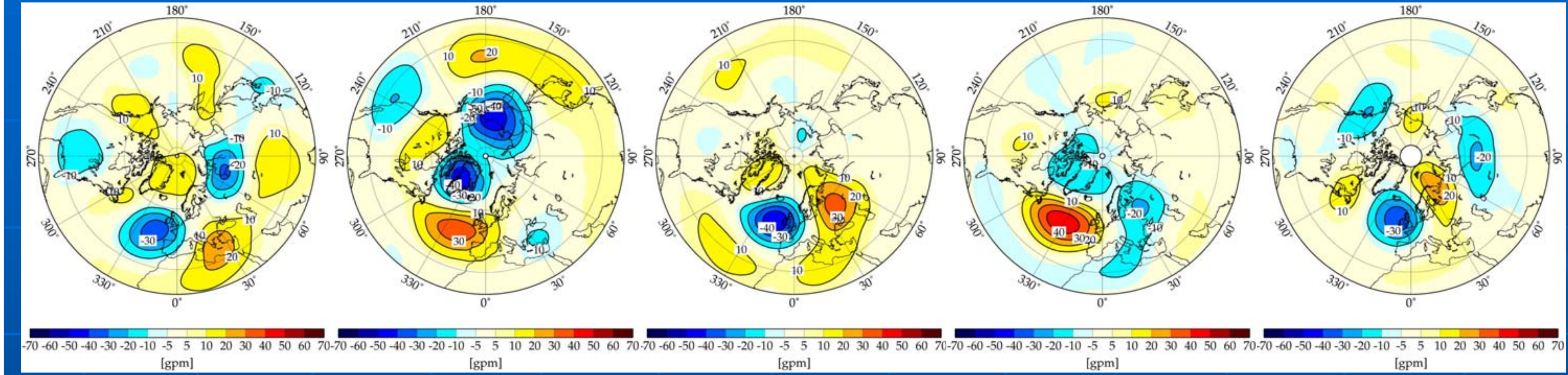

ERA40 NCEP

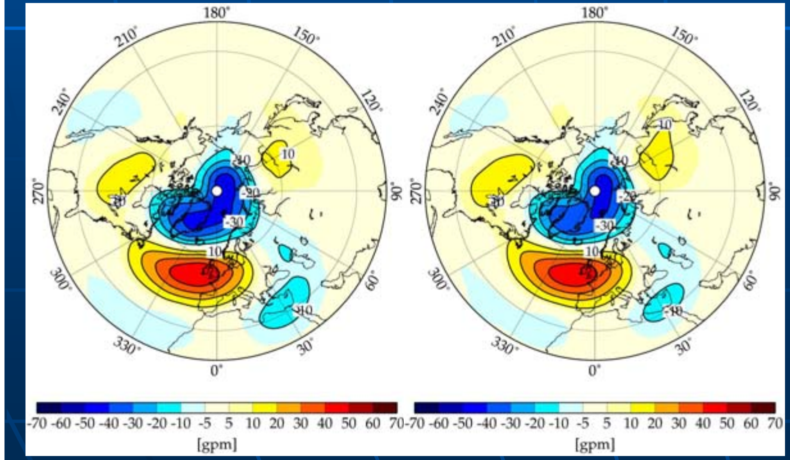

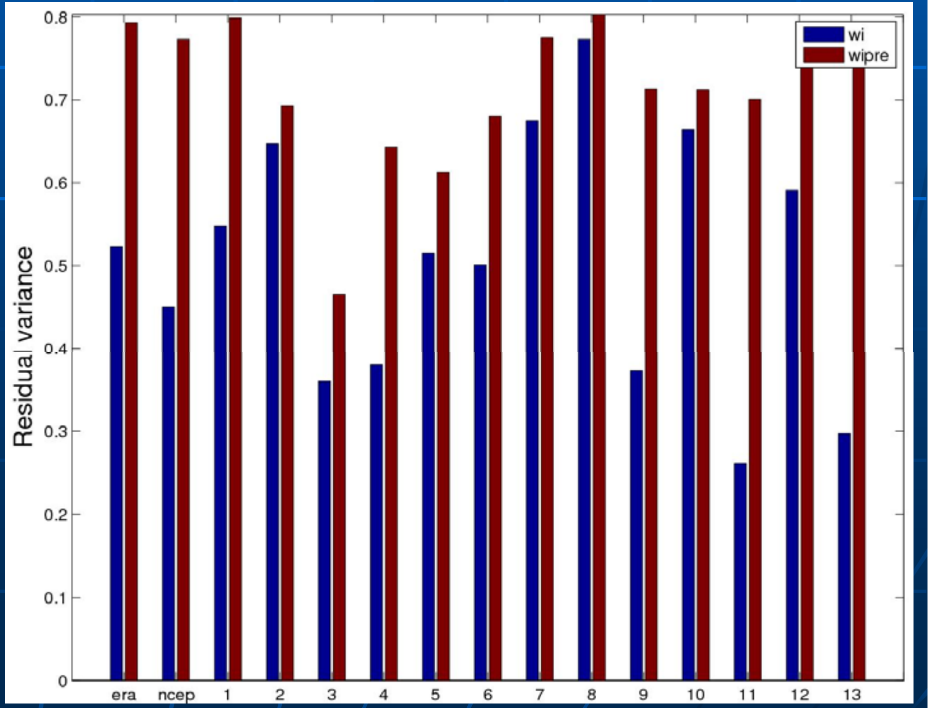

Potentially Predictable Patterns, 13 AMIP models

PNA, Period 1979-1999

MPI-ECHAM5/OM1 NCAR-PCM UKMO-HadGEM MIROC-MEDRES IAP

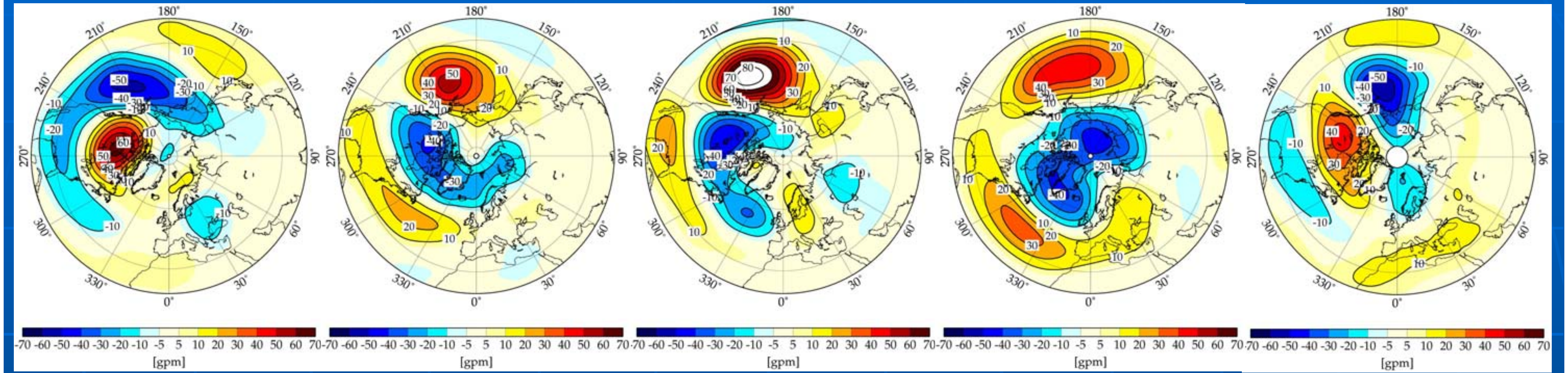

ERA40 NCEP

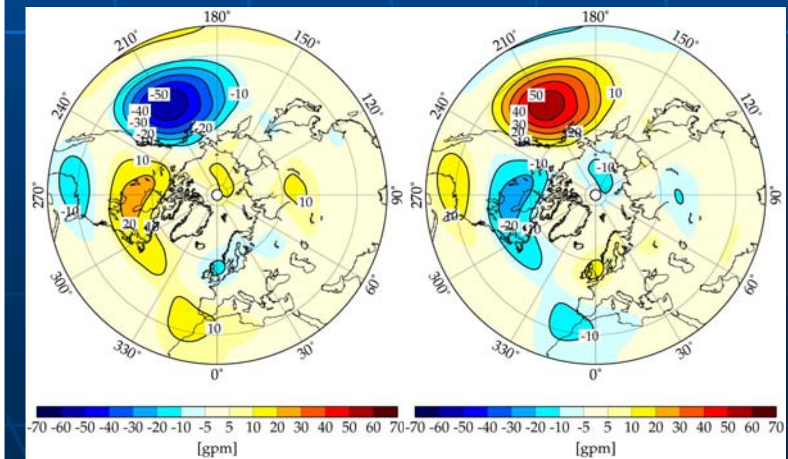

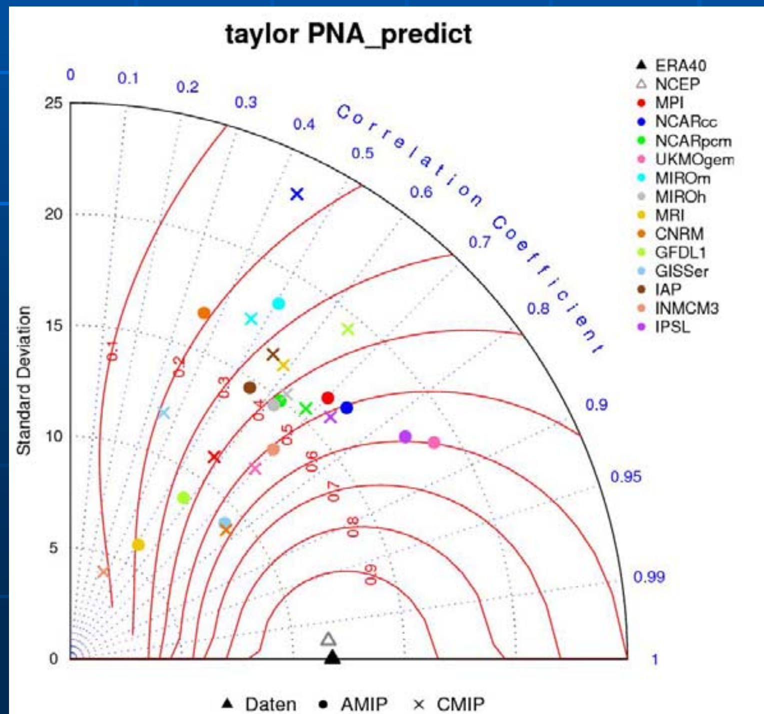

Potentially Predictable Patterns, 13 AMIP models

PNA, Period 1979-1999

MPI-ECHAM5/OM1 NCAR-PCM UKMO-HadGEM MIROC-MEDRES IAP

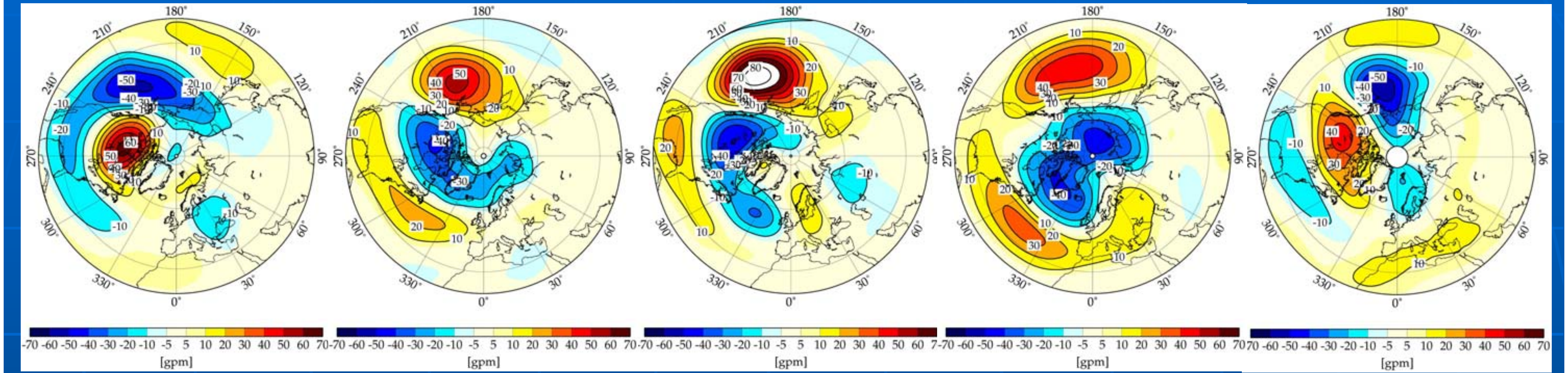

ERA40 NCEP

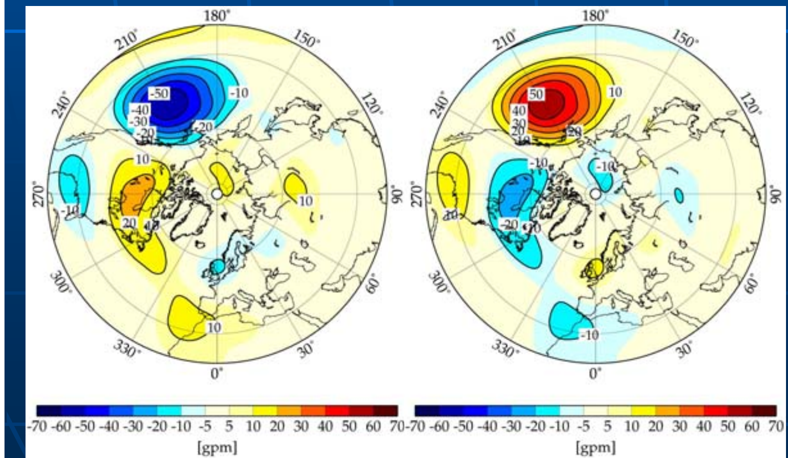

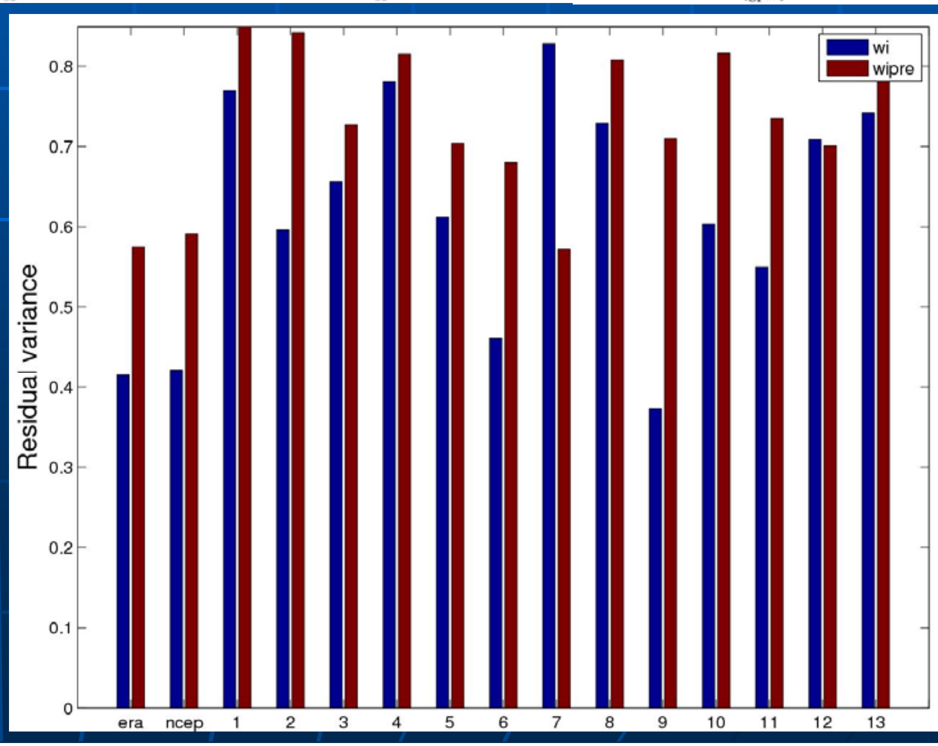

Pattern Metrics, 23 CMIP models, 1958-1999

Seasonal Teleconnection Patterns

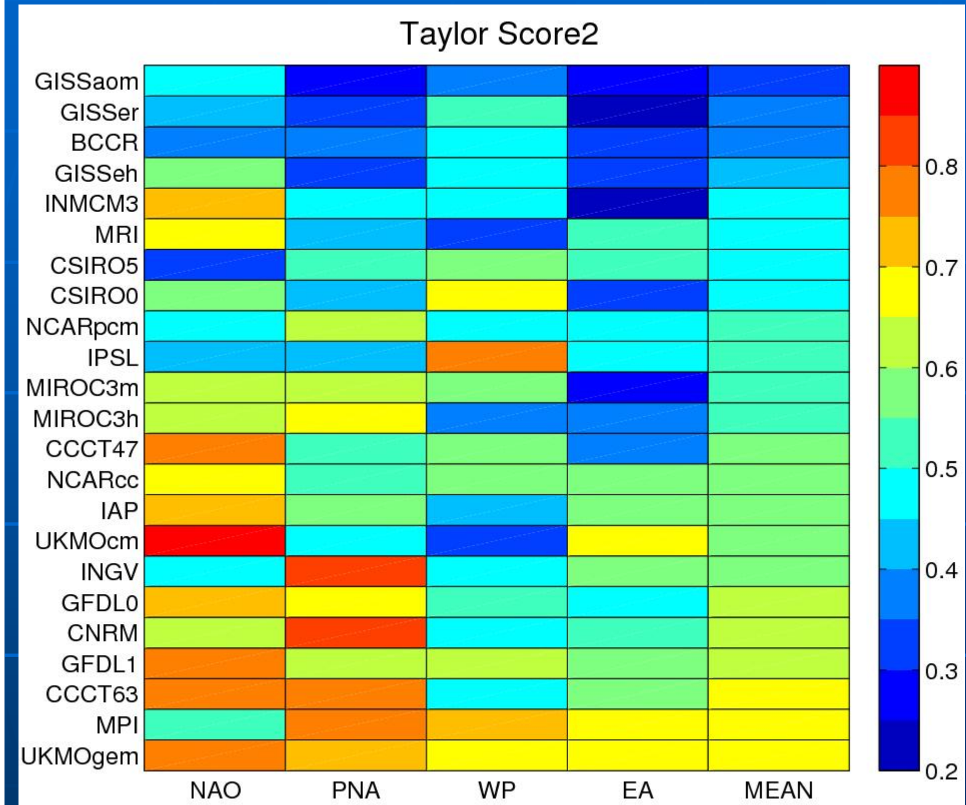

Potentially Predictable Patterns

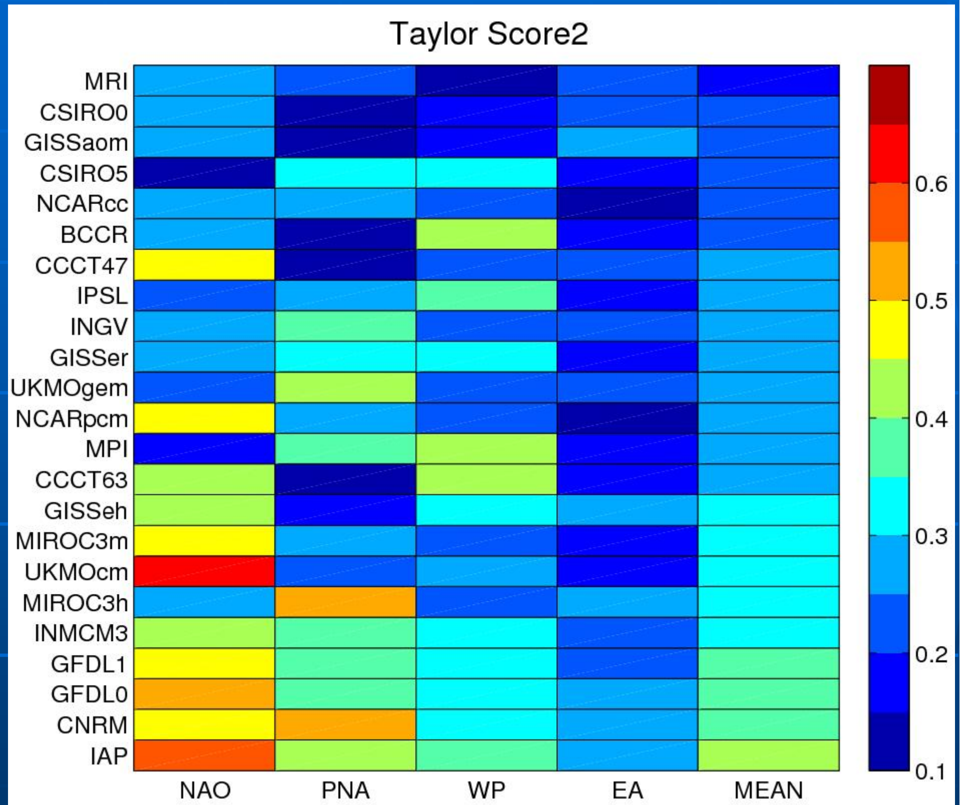

Pattern Metrics, 13 AMIP models, 1979-1999

Seasonal Teleconnection Patterns   Potentially Predictable Patterns

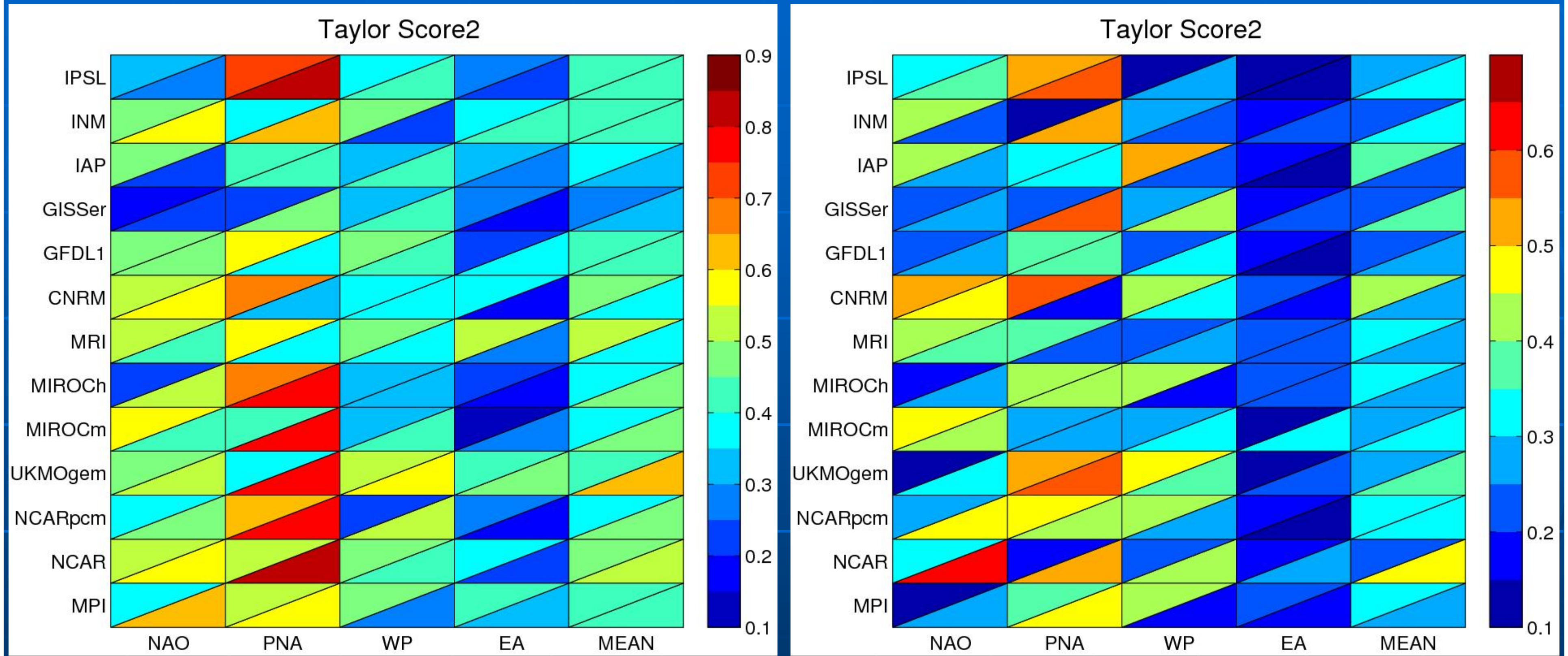

Upper triangle: CMIP simulations
Lower triangle: AMIP simulations

Summary and Conclusions

- Potentially Predictable Patterns determined with the method of Zheng and Fredriksen (2004)
- Potentially Predictable Patterns have horizontal structures similar to the known teleconnection patterns
- Potentially Predictable Patterns are more closely related to external forcing and low-frequency internal dynamics
- Tool for model validation

- GCMs are less capable to reproduce potentially predictable patterns then to reproduce seasonal teleconnection patterns
  → Why? (Understanding of underlying physics)
- Realistic boundary forcing
  → significant improvement only for PNA-like patterns

Outlook

- Influence of stronger external forcing on Potentially Predictable Patterns

  → Analyses of Scenario runs

Slow Patterns, NH 20-90ºN PNA, SRESA1B period 2000-2049

MPI-ECHAM5/OM1 NCAR-PCM UKMO-HadGEM MIROC-MEDRES IAP

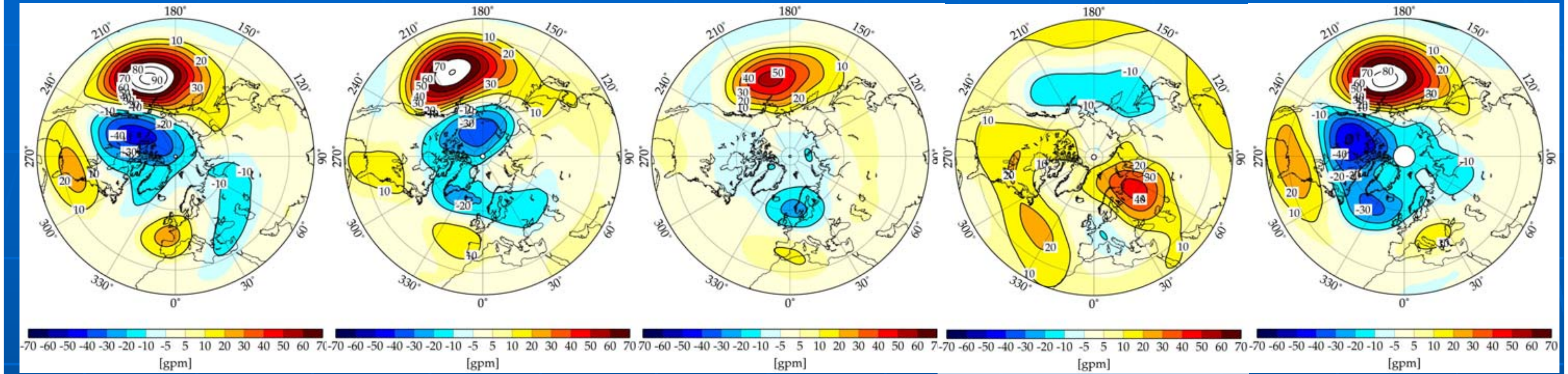

ERA40

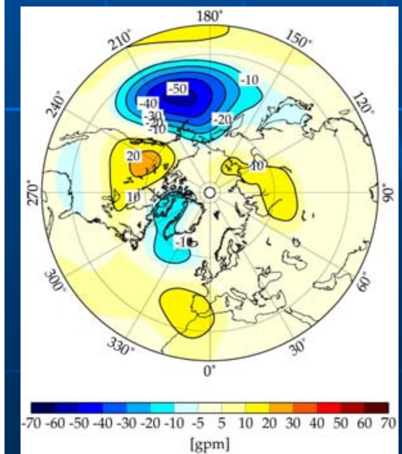

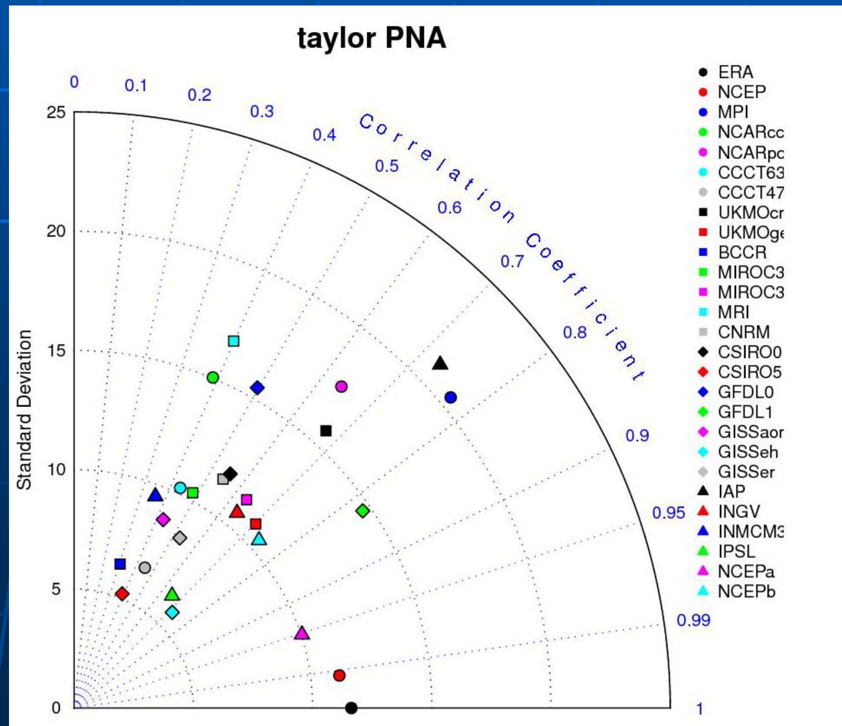

Slow patterns, NH 20-90°N PNA, SRESA1B period 2050-2099

MPI-ECHAM5/OM1 NCAR-PCM UKMO-HadGEM MIROC-MEDRES IAP

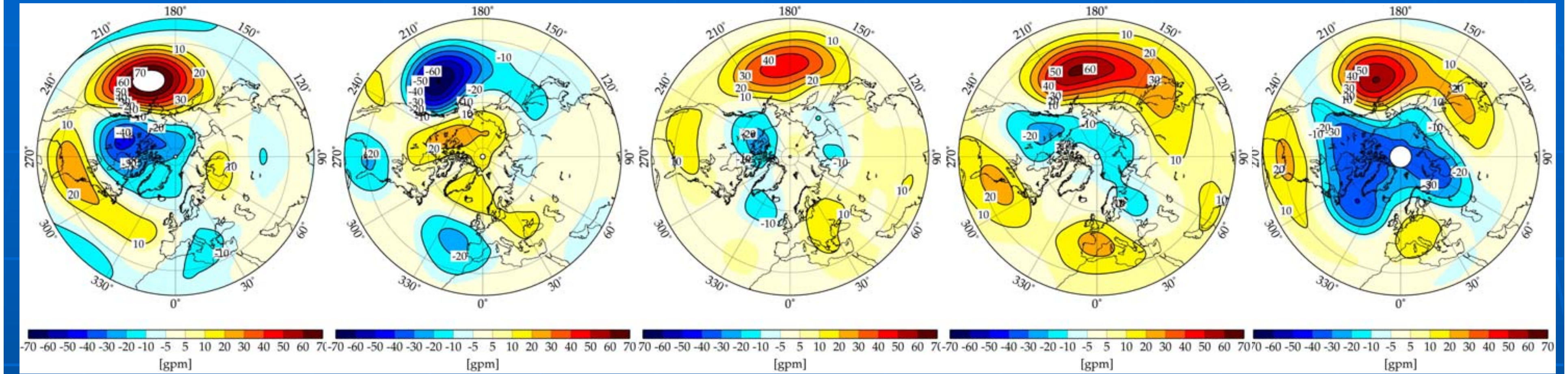

ERA40

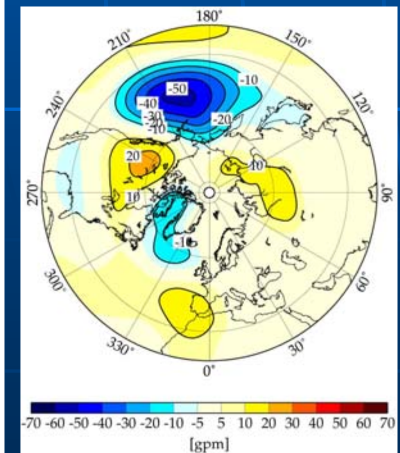

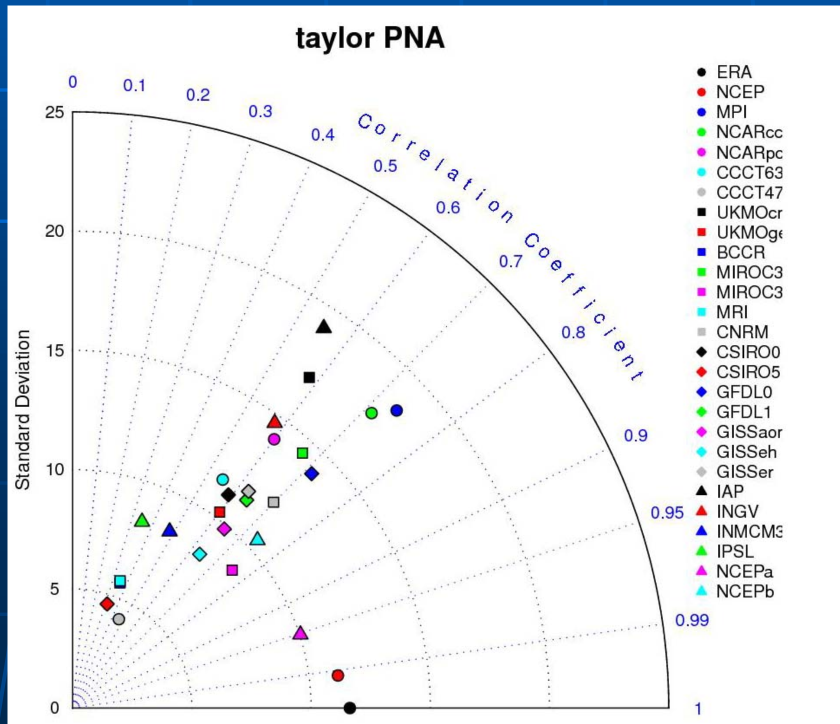

Slow patterns, NH 20-90^{o}N PNA, SRESA1B

2000-2049 2050-2099

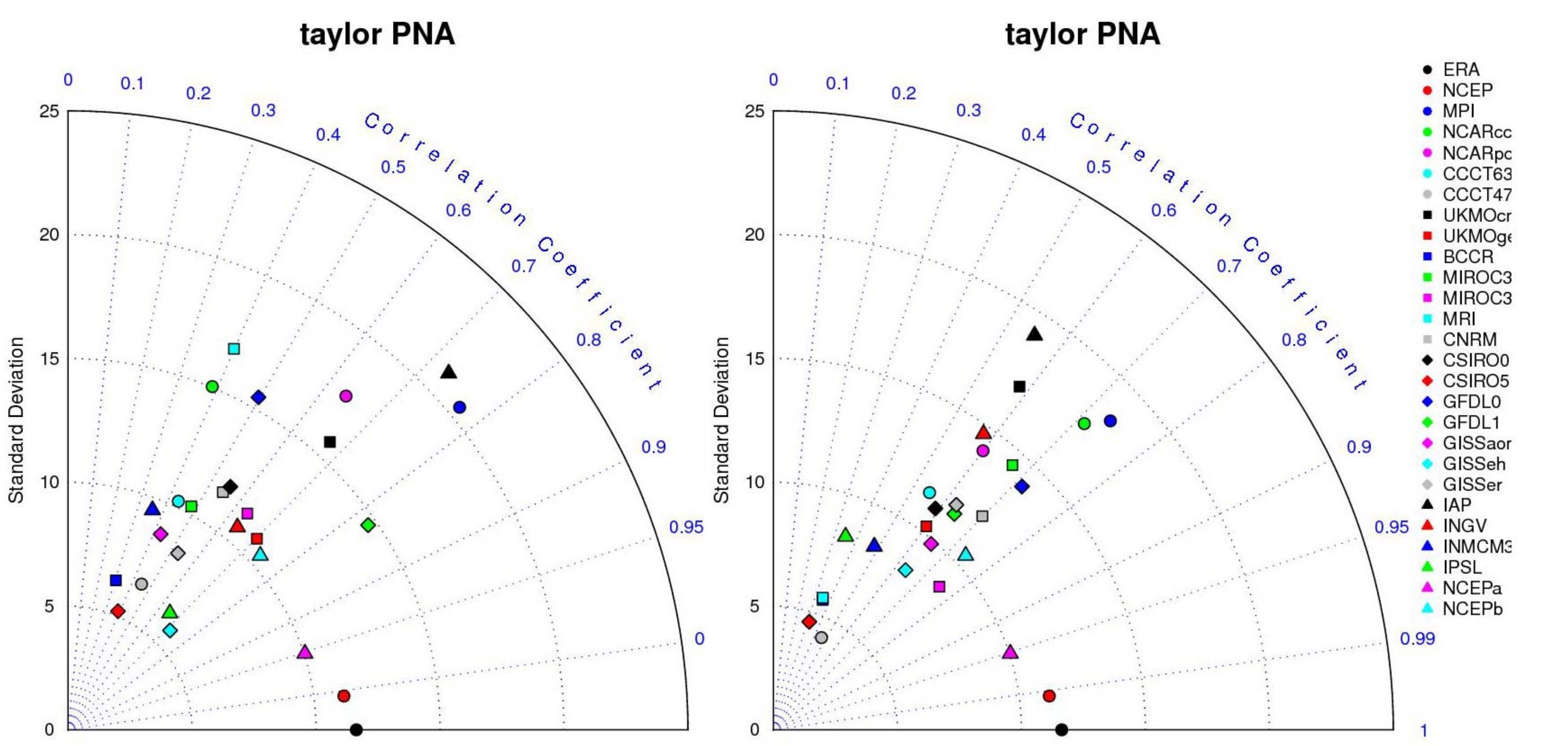

Outlook

- Influence of stronger external forcing on Potentially Predictable Patterns
  → Analyses of Scenario runs

- Separation of externally forced componant and internally generated componant of interannual to decadal climate variability
  → Application of two-way ANOVA model for
  the analyses of ensemble simulations (Zheng et al., QJRMS, 2009)

- Understanding of dynamical mechanisms underlying the variability patterns